https://doi.org/10.5194/egusphere-2025-3536
Preprint. Discussion started: 4 January 2026

Evaluation of HNO_3, SO_2, and NH_3 in the Surface Tiled Aerosol and Gaseous Exchange (STAGE) option in the Community Multiscale Air Quality Model version 5.3.2 against field-scale, *in situ* and satellite observations

Jesse O. Bash[1], John T. Walker[1,a], Zhiyong Wu[1,b], Ian C. Rumsey[1], Ben Murphy[1], Christian Hogrefe[1], Kathleen M. Fahey[1], Havala O.T. Pye[1], Matthew R. Jones[2], K. Wyat Appel[1], Mark Shephard[3], Najwa I. Alnsour[4,c], Karen E. Cady-Periera[5]

[1] U.S. Environmental Protection Agency, Research Triangle Park, NC, USA
[2] Center for Ecology and Hydrology, Edinburgh, Scotland, UK
[3] Air Quality Research Division, Environment and Climate Change Canada, Toronto, Ontario, Canada
[4] North Carolina State University, NC, USA
[5] Atmospheric and Environmental Research, Inc., Lexington, MA, USA
[a] Now at U.S. Forest Service, Otto, NC, USA
[b] Now at RTI International, Research Triangle Park, NC, USA
[c] Now at USDA, Mandan, ND, USA

Correspondence to: Ian C. Rumsey (rumsey.ian@epa.gov)

Abstract. The Surface Tiled Aerosol and Gaseous Exchange (STAGE) model was developed for estimating dry deposition and bidirectional exchange for field-scale applications and use within the CMAQ v5.3.2 regional scale model. The model was evaluated against micrometeorological flux measurements of NH_3, HNO_3, and SO_2 at a managed grassland and NH_3 in a cultivated corn (*Zea Mays*) field. When using field-scale observations for soil and vegetation NH_3 compensation points, modelled fluxes for all species agreed well, within or near the reported measurement uncertainty. However, when using the CMAQ v5.3.2 values for NH_3 emission potentials at the Duke Forest grassland site, the model estimated mean net deposition rate was 1.3 ng m^{-2} h^{-1} while the observed mean NH_3 evasive flux was 8.4 ng m^{-2} h^{-1}. Modelled NH_3 concentration fields evaluated against Cross-Track Infrared Sounder (CrIS) satellite observations indicates a broad underestimation of NH_3 concentrations by approximately 1 to 2 ppb in the U.S. Great Plains. The results from the grassland field data and indicates that there is likely an underestimation of the evasive NH_3 flux in grassland sites due to the model's default tabular values of the vegetation/litter NH_4^+ concentrations. The STAGE's model sensitivity to soil and vegetation emission potentials indicates that regional scale model results for NH_3 can be further improved with additional micrometeorological flux and vegetation and soil chemistry measurements over different land use types, soil types, and vegetation phenological stages.

https://doi.org/10.5194/egusphere-2025-3536
Preprint. Discussion started: 4 January 2026

1 Introduction

Ammonia (NH_3), sulfur dioxide (SO_2) and nitric acid (HNO_3) are gaseous precursors to atmospheric particulate matter formation (Seinfeld and Pandis, 1998) which is deleterious to human health and of global importance (Burnett et al., 2018). In addition to adverse human health impacts the atmospheric deposition of these pollutants contributes to soil and water acidification and excess nutrient loading to sensitive ecosystems (Greaver et al., 2012). In the U.S., oxidized forms of nitrogen and sulfur are regulated under the U.S. National Ambient Air Quality Standards (NAAQS) established under the Clean Air Act Amendments (US Congress 1990; USEPA 2020a). The exchange of atmospheric aerosols and trace gases between the atmosphere and biosphere is an essential process in the source, transport and fate of atmospheric pollutants and represents an important vector of ecosystem and human health exposures (Eschelman and Sabo, 2016; Greaver et al., 2012; Burnett et al., 1998; Galloway et al., 2020). In regional and global chemical transport models, evasive/emission and dry deposition components of the net flux are typically treated separately, often with different parameterizations and assumptions, despite being governed by many of the same biogeochemical and physical processes (Saylor and Hicks, 2016). Field-scale models have been developed that consistently parameterize the net flux of pollutants for a limited number of atmospheric trace gases (Nemitz et al., 2001, Persone et al., 2009, Massad et al., 2010, Stella et al., 2011). In regional and global scale applications, these flux/bidirectional exchange parameterizations have only been applied to mercury (Hg) and NH_3 (Zhang et al., 2010; Bash 2010; Wichink Kruit et al., 2012; Bash et al., 2013; Wang et al., 2014; Zhu et al., 2015) despite many volatile organic carbon (VOC; e.g., Millet et al., 2018) and nitrogen compounds (e.g. Skiba et al., 1999; Wu et al., 2019) exhibiting both evasive and deposition fluxes depending on environmental and biological conditions.

Models developed to simulate field-scale fluxes often include both evasive and deposition fluxes and typically employ an electrical resistance analog to drive the estimated fluxes in bulk, e.g., big leaf, (Nemitz et al., 2001), multi-layer Eulerian (e.g. Wolfe and Thornton 2011, Bash et al., 2010), or Lagrangian frameworks (e.g. Raupauch 1989). However, regional and global scale chemical transport models typically parameterize deposition and emission processes separately with deposition being typically described using a resistance model analog (e.g. Pleim and Ran 2011) and emissions typically modelled with a bottom-up approach using emissions factors (Olaguer 2017). These different approaches for modelling emissions and deposition arise due to the differing needs of science and regulatory applications. For example, field-scale models are typically used to illuminate processes governing the exchange of trace pollutants, while regional-scale models like CMAQ are used, among other purposes, to support environmental legislation like the National Ambient Air Quality Standards, NAAQS (Clean Air Act Amendment, U.S. Congress, 1990) and the Total Maximum Daily Load (TMDL) assessments (Clean Water Act, U.S. Congress, 1972) or critical loads (Byrne 2015). Emissions factors will likely continue to be used to support the accounting of anthropogenic emissions regulated under the NAAQS. However, natural and evaporative emissions where the flux is determined by the production of the trace gas in the environmental media, e.g., soil NO_x, NH_3 from agricultural sources, and biogenic VOCs, etc., can be modelled using gradient based methods as advocated by Saylor and Hicks (2016).

https://doi.org/10.5194/egusphere-2025-3536
Preprint. Discussion started: 4 January 2026

In versions of CMAQ prior to v5.3.2, the parametrization for NH_3 bidirectional exchange added canopy elements to the effective aerodynamic resistance, i.e., adding half the in-canopy resistance to the aerodynamic resistance, to effectively model observations of NH_3 fluxes over a corn canopy (Pleim et al., 2013). While this simulated fluxes over an agricultural field well, it is not well suited to be applied to species that deposit quickly, e.g., HNO_3, as it results in smaller dry deposition velocities than the typically observed values largely constrained by the aerodynamic and quasi-laminar boundary layer resistances (Nguyen et al., 2015) and was therefore not applied to other modelled species. This resulted in two parallel resistance models, one for NH_3 bidirectional exchange and one for all other species implemented in CMAQ. Additionally, observations of deposition velocities exhibit a large range across forested, short vegetation and smooth surfaces (Schrader and Brümmer 2014, Zhang et al., 2002). The need for land use specific deposition fluxes from regional scale models is being driven by advancements in the identification of vegetation species and plant functional type differences in critical loads responses to nitrogen and sulfur deposition (Clark et al., 2019) and the land use specific transport effectiveness of deposited nitrogen in the watershed to the surface waters where the impact of nutrient enrichments are driving Total Maximum Daily Load (TMDL) assessments (Hood et al., 2021). In a gridded modelling system, a land use specific, or tiled, approach is used as the vastly different nitrogen budget of agricultural ecosystems relative to other land use types can perturb the entire grid cell nitrogen budget when using a bulk parameterization. Here we modify and generalize the commonly used resistance model developed by Nemitz et al. (2001) for field-scale modelling of bidirectional turbulent fluxes (Massad et al., 2010; Personne et al., 2009; Stella et al., 2011; Hansen et al., 2017) for use in modelling field scale trace gas fluxes and in regional scale air-quality applications. This parameterization is available in CMAQ v5.3 and later releases as the Surface Tiled Aerosol and Gaseous Exchange (STAGE) deposition option (Galmarini et al., 2021; Appel et al., 2021).. This dry deposition framework is applied to all modelled atmospheric gases in CMAQ, evaluate against observed field-scale NH_3, SO_2, and HNO_3 fluxes, and, on a regional scale, against monitoring networks and satellite NH_3 observations.

2 Methods and Materials

2.1 STAGE resistance parameterization

The STAGE deposition option closely follows the widely used Massad et al. (2010) and Nemitz et al. (2001) parameterizations, modified to include the option for a cuticular compensation point and is unique in CMAQ as it employs the same resistance model for bidirectional and unidirectional exchange, Figure 1.

https://doi.org/10.5194/egusphere-2025-3536
Preprint. Discussion started: 4 January 2026

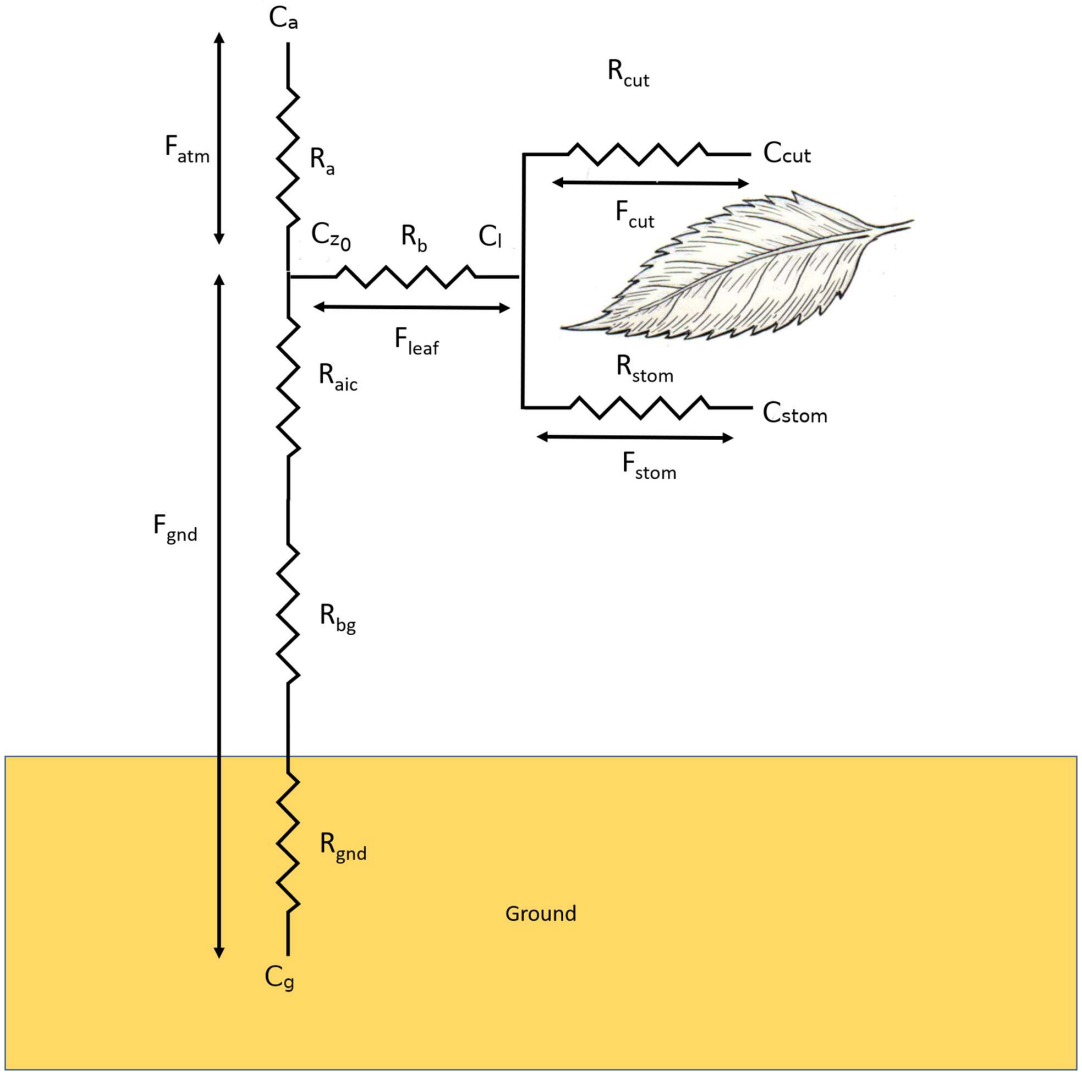

Figure 1. STAGE resistance wire diagram modified from Nemitz et al. 2001 to include non-zero compensation points for leaf cuticular surfaces. Leaf image adapted from Pearson Scott Foresman / Public domain https://commons.wikimedia.org/wiki/File:Acuminate_Leaf_(PSF).jpg

The flux of a trace gas between the atmosphere and surface is modelled following Nemitz et al. (2001) as:

$$F_t = -\frac{C_a - C_{z0}}{R_a} \quad (1)$$

https://doi.org/10.5194/egusphere-2025-3536
Preprint. Discussion started: 4 January 2026

where, C_a is the ambient atmospheric concentration, C_{z0} is the compensation point concentration at the sum of the aerodynamic displacement height (d) and roughness length (z_0) and R_a is the aerodynamic resistance. The compensation point is estimated using a two-layer, soil and canopy model following Nemitz et al. (2001).

$$c_{z0} = \frac{\frac{C_a}{R_a} + \frac{C_l}{R_{b,v}} + \frac{C_g}{R_{gnd}}}{(R_a)^{-1} + \left(R_{b,v}\right)^{-1} + \left(R_{gnd}\right)^{-1}} \quad (2)$$

C_l is the compensation point at the leaf, C_g is the soil air-pore space concentration, $R_{b,v}$ is the leaf quasi-laminar boundary layer resistance following Massad et al (2010), and R_{gnd} is defined as the sum of the in-canopy resistance, soil quasi-boundary layer resistance and soil resistance (R_{gnd}=R_{inc}+$R_{b,s}$+R_{soil}). C_l is estimated by solving for the exchange between the canopy compensation point and the atmosphere, stomata, cuticle and ground following Kirchhoff's current law (see Nemitz et al., 2000). C_l is solved from this system of equations following the work of Nemitz et al. (2001) with the addition of a cuticular compensation point:

$$C_l = \frac{\frac{C_a}{R_a R_{b,v}} + \frac{C_{stom}}{R_a R_s + R_{b,v} R_s + R_{gmd} R_s} + \frac{C_{cut}}{R_a R_{cut} + R_{b,v} R_{cut} + R_{gnd} R_{cut}} + \frac{C_g}{R_{b,v} R_{gnd}}}{\left(R_a R_{b,v}\right)^{-1} + (R_a R_s)^{-1} + (R_a R_{cut})^{-1} + \left(R_{b,v} R_s\right)^{-1} + \left(R_{b,v} R_{cut}\right)^{-1} + \left(R_{b,v} R_{gnd}\right)^{-1} + \left(R_{gnd} R_s\right)^{-1} + \left(R_{gnd} R_{cut}\right)^{-1}} \quad (3)$$

where, C_{stom} is the gaseous compensation point concentration in the leaf mesophyll, C_{cut} is the gaseous compensation point concentration at the cuticular surface, R_s is the sum of stomatal and mesophyll resistances, and R_{cut} is the cuticular resistance. The resistance parameterization algorithms and references are listed in Table 1.

https://doi.org/10.5194/egusphere-2025-3536
Preprint. Discussion started: 4 January 2026

Table 1, modelled resistance the form of the resistance functions and references used in the STAGE model.

Resistance	Formulation	Reference
r_a	$\frac{\varphi_h}{u_* k}\left[ln\left(\frac{z}{z_0}\right) - \psi_h\left(\frac{z}{L}, \frac{z_0}{L}\right)\right]$	Pleim and Ran, 2011
r_b	$\frac{\nu}{D_i}\left(\frac{c\, l\, u_*}{LAI^2 \nu}\right)^{\frac{1}{3}} \frac{1}{u_*}$	Jensen and Hummelshøj, 1995 Massad et al., 2010
r_{bg}	$\frac{\frac{\nu}{D_{g,i}} - \ln\left(\frac{\delta_0}{z_1}\right)}{k\, u_{*,g}}$	Massad et al., 2010 Nemitz et al., 2001
$r_{cut,dry}$	$R_{cut,dry} = \frac{a_0 r_{cut0}}{Rx_i}$	Pleim and Ran, 2011
$r_{surf,wet}$	$R_{surf,wet} = \left(\frac{l_{wat}}{D_{g,i}} + \frac{4}{3\sqrt{\frac{4RT}{MW_i \pi}}\alpha_i}\right)\left(1 + \frac{1}{l_{wat} H_i}\right)$	This work, adapted from Fahey et al. (2017)
$r_{stom,i}$	$R_{stom,i} = \frac{D_{g,wat}}{D_{g,i}} R_{stom,wat}$	Pleim and Ran, 2011
$r_{mes,i}$	$R_{mes,i} = \frac{1}{LAI\left(\frac{H_i}{3000} + 100 f_i\right)}$	Wesely, 1989 Pleim and Ran, 2011
r_{aic}	$R_{aic} = R_a\left(e^{\frac{LAI}{2}} - 1\right)$	This work following Raupach (1989)
r_{gnd}	$R_{gnd,dry} = \frac{a_0 R_{gnd0}}{Rx_i}$	Pleim and Ran, 2011
r_{snow}	$R_{snow} = \frac{a_0 R_{snow0}}{Rx_i}$	Pleim and Ran, 2011
$r_{snow,diff}$	$R_{snow,diff} = 10$	Pleim and Ran, 2011

The cuticular and soil pathways can be either dry, wet or snow covered where each pathway is assumed to be parallel.

$$R_x = \frac{f_{dry}}{R_{x,dry}} + \frac{f_{wet}}{R_{wet}} + \frac{f_{snow}}{R_{snow}} \quad (4)$$

where R_x is either the cuticular or soil resistance, f_{dry}, f_{wet} and f_{snow} are the ratio of dry, wet or snow covered surface to the surface area constrained by $f_{dry} + f_{wet} + f_{snow} = 1$, $R_{x,dry}$ is the resistance of the modelled species to dry soil or cuticular surfaces, R_{wet} is the resistance of the modelled species to deposition to surface bound water droplets, and R_{snow} is the resistance of the model species to deposition to snow covered surfaces.

If the soil, cuticular and stomatal compensation points are zero, then the transfer coefficient in this resistance model reduces to a typical dry deposition model similar in form to Clifton et al. (2020):

https://doi.org/10.5194/egusphere-2025-3536
Preprint. Discussion started: 4 January 2026

$$V_d = \left[R_a + \frac{1}{\frac{1}{R_{b,v} + \frac{1}{\frac{1}{R_{cut}} + \frac{1}{R_s}}} + \frac{1}{R_{gnd}}} \right]^{-1} \quad (5)$$

where V_d is the dry deposition velocity and the flux can be modelled as:

$$F_t = -C_a V_d \quad (6)$$

This allows for the use of this resistance model framework for species that exhibit bidirectional exchange, e.g., NH_3, and species that do not, e.g., HNO_3, and has the advantage of having a consistent set of assumptions regarding the deposition and bidirectional exchange of pollutants. Similarly, the evasive portion of the flux in the CMAQ implementation is estimated following Bash et al. (2013) to separate evasive and deposition fluxes.

$$F_t = -C_a V_d + \frac{C_{z0}(C_a = 0.0)}{R_a} \quad (7)$$

Splitting deposition and emission processes allows for the application of source apportionment tools to species that exhibit bidirectional exchange and estimate emission sensitivities, e.g., the sensitivity of ambient NH_3 to agricultural fertilizer applications.

2.1.1 Model generalizations

This work largely follows the modelling work of Massad et al (2010) and Nemitz et al. (2001) for most of the resistance algorithms describing physical transport processes and for NH_3 exchange (Table 1). Most of the other chemically dependent resistance parameterizations follow CMAQ M3Dry parameterization (Pleim and Ran, 2011). However, several modifications were made to generalize the resistance model for application to all CMAQ's modelled species, implementation into a regional scale model, and to harmonize parameterizations and assumptions used in other modules of the CMAQ modelling system. Additionally, a method for determining the cuticular resistance for non-ionic organic trace gases was developed based on the species vapor pressure and is analogous to aerosol partitioning, Supplemental material S1, but is not presented in the evaluation due to a lack of observational data. The cuticular resistances of all other trace gases are modelled following Pleim and Ran (2011).

2.1.2 Resistance to wet surfaces

Prior to CMAQ v5.3, the parameterization of deposition to wet canopy surfaces is effectively an instantaneous diffusion into the canopy water. Here we adapted the mechanisms used to model diffusion and adsorption of trace gasses into water droplets in CMAQ's extendable aqueous-phase chemistry option (AQCHEM-KMT) (Fahey et al., 2017).

https://doi.org/10.5194/egusphere-2025-3536
Preprint. Discussion started: 4 January 2026

$$k_{mt,i} = \left(\frac{r^2}{3D_{g,i}} + \frac{4r}{3\sqrt{\frac{8RT}{MW_i\pi}}\alpha_i} \right)^{-1} \quad (8)$$

Where $D_{g,i}$ is the gaseous diffusivity and α_i is the bulk accommodation coefficent for the modelled species, *i*. Most vascular, non-aquatic plant leaves are hydrophobic and wetted surfaces will be composed of roughly spherical droplets (Barthlott et al., 2016). If we choose the droplet radius, *r*, as the characteristic length, then this can be converted to a resistance by

$$r_{mt,i} = \left(\frac{r^2}{3D_{g,i}} + \frac{4r}{3\sqrt{\frac{8RT}{MW_i\pi}}\alpha_i} \right) r^{-1} = \left(\frac{r}{3D_{g,i}} + \frac{4}{3\sqrt{\frac{8RT}{MW_i\pi}}\alpha_i} \right) \quad (9)$$

Then the overall resistance to cuticular deposition using the two-film theory of Liss and Slater (1974) is:

$$R_{wet,i} = r_{mt,i} + \frac{r_{mt,i}}{H} \quad (10)$$

where H is the dimensionless Henry's constant. The radius of the water droplet, r, is taken as a constant of 1.9×10^{-4} m. This assumes that the wet leaf surfaces have an RH of 100% and using the leaf wetness model of van Hove and Adema (1996) and a contact angle of 90°, uniform wetness on the canopy and spherical droplets on the hydrophobic leaf surfaces. This adds a mass accommodation term in addition to solubility into the surface resistance resulting in additional physical limits to the maximum deposition rate of highly soluble compounds.

Burkhardt *et al.* 2009 derived the moisture depth as a function of RH using observed leaf wetness and Brunauer-Emmett-Teller, BET, theory (Brunauer et al., 1938). They report a maximum depth of 100 µm similar to the observations of van Hove and Adema (1996). These studies give the specific liquid volume per leaf area, $\frac{w_L}{LAI}$.

From Burkhardt et al 2009, the fractional leaf wetness derived empirically from observations is:

$$LW = 3.68x10^{-4}e^{7.9\,RH} \quad (11)$$

where RH is the humidity ranging from 0 to 1. Then the depth of liquid water in meters using the BET theory with empirical coefficients to match the results of van Hove and Adema (1996) becomes:

$$w_L = 3.13x10^{-7} LAI\, e^{5.767\,RH} \quad (12)$$

Assuming a contact angle of 90°, uniform wetness on the canopy and spherical droplets on the hydrophobic leaf surfaces the radius of the droplets on the leaves, *r*, is:

https://doi.org/10.5194/egusphere-2025-3536
Preprint. Discussion started: 4 January 2026

$$r = \frac{6\, w_L}{\pi LAI} \tag{13}$$

2.1.3 In-canopy aerodynamic resistance

Here the in-canopy aerodynamic resistance is estimated by integrating the in-canopy eddy diffusivity from the ground surface to the canopy top, H_c, using the attenuation coefficient of Yi (2008):

$$R_{inc} = \int_0^{H_c} \frac{dz}{K_t} \tag{14}$$

where R_{inc} is the in-canopy aerodynamic resistance, H_c is the canopy height, and K_t is the eddy diffusivity. Following K theory, the eddy diffusivity can be estimated from the surface friction velocity, u_*, and the mean wind speed, $\bar{U}$, gradient.

$$K_t = u_*^2 \left(\frac{d\bar{U}}{dz}\right)^{-1} \tag{15}$$

Following Yi 2008 the wind speed in the canopy can be modelled as:

$$\bar{U}(z) = \bar{U}(H_c) e^{\left[\frac{LAI}{2}\left(\frac{z}{H_c}-1\right)\right]} \tag{16}$$

where z is the height above the soil and LAI is the leaf area index. Combining eqations 14, 15 , 16 and defining the aerodynamic resistance as $R_a = \frac{\bar{U}(H_c)}{u_*^2}$.

$$R_{inc} = \mathrm{R}_a \left(e^{\left[\frac{LAI}{2}\right]} - 1\right) \tag{17}$$

This result can also be derived if the cumulative LAI is chosen as the vertical coordinate assuming a uniform LAI distribution. This is similar to the parameterization in Shuttleworth and Wallace (1985) using the momentum attenuation coefficient from Yi (2008).

2.2 NH_3 bidirectional exchange

Several updates were made to the soil processes in the NH_3 bidirectional exchange algorithms for the STAGE deposition option implementation in CMAQ v5.3.2. The first was specifying a maximum diffusive length in estimating the resistance to emissions or deposition to soil surfaces. Earlier versions of CMAQ used the 1 cm soil layer depth of the P-X land surface model (Pleim and Xui 1995). This was changed to 2 cm to be consistent with the measurements used to derive the diffusive model (Kondo et al., 1990) and to fall in the middle of the dry layer thickness range of 1 to 3 cm reported by Swenson and Lawrence (2014).

Releases of CMAQ before v5.3 estimated that 55% of the soil ammonium was in the soil water solution based on measurements with extractants with variable ionic strengths (Cooter et al., 2010). Here, we employ the non-linear ammonium sorption capacities to estimate the NH_4^+ in the soil water solution and available for evasion (Venterea et al., 2015).

https://doi.org/10.5194/egusphere-2025-3536
Preprint. Discussion started: 4 January 2026

$$NH_{4,s}^{+} = \frac{\mu\, NH_{4,aq}^{+}}{K + NH_{4,aq}^{+}} \quad (18)$$

where $NH_{4,s}^{+}$ is the ammonium sorbed to soil particles, $NH_{4,aq}^{+}$ is the ammonium in the soil water solution, μ is the maximum soil sorption capacity and K is the $NH_{4,aq}^{+}$ concentration where $NH_{4,s}^{+} = 0.5\mu$, Table 2.

Table 2. Tabular CMAQ v5.3 model parameters and measured median values

Measurement period (units)	CMAQ v5.3.2 Grassland	Duke Forest, NC	CMAQ v5.3.2 Agriculture	Lillington, NC
Soil *Γ (dimensionless)*	20	869	85,294	85,294
Litter *Γ (dimensionless)*	NA	144	NA	NA
Vegetation *Γ (dimensionless)*	247	2,741	Function of soil NH_4 (2,750)	153.5
Dew *Γ (dimensionless)*	0	1	0	4565
Minimum Stomatal resistance (s/m)	100	Not estimated used CMAQ value	70	154
Venterea μ (mg kg^{-1})	550	426 (KCl) 585 (H_2O)	550	Not measured
venterea K (mg L^{-1})	345	124 (KCl) 327 (H_2O)	345	Not measured

2.3 Site descriptions and box model simulations

Field-scale flux data collected from July 5th to November 23rd 2012 at a managed, unfertilized 15 ha grass field at the Duke Forest Blackwood Division, NC (35.58° N, 79.05° W ; Rumsey and Walker, 2016) from July 5th to November 23rd 2012 and at a 200 ha fertilized corn field near Lillington, NC (35.38° N, 78.78° N; Walker et al., 2013) from May 29th to June 29th 2007 were used to evaluate the STAGE model. Micrometeorological flux measurements of NH_3 and latent heat available at both sites and HNO_3 and SO_2 fluxes are available at the Duke Forest site were used to evaluate modelled fluxes. At Lillington, air concentrations and above-canopy vertical gradients of NH_3 were measured with a continuous flow "AMANDA" (Ammonia Measurement by ANnular Denuder sampling with online Analysis; Wyers et al., 1993) wet denuder system and fluxes were determined using the modified Bowen ratio method (Meyers et al., 1996). At Duke Forest, air concentrations and above-canopy vertical gradients of HNO_3, SO_2 and NH_3 were measured using the Monitor for AeRosols and GAses in ambient air (MARGA, Metrohm-Applikon, the Netherlands) (Rumsey et al., 2014) and fluxes were determined using the aerodynamic gradient methods (Thomas et al., 2012). At both sites, eddy covariance was used to determine fluxes of latent heat using an open-path infrared gas analyzer (LI-COR 7500, LI-COR, Inc., Lincoln Nebraska). LAI was not measured during the flux campaign at Duke Forest but there were measurements of canopy height and LAI (LAI-2000, LI-COR, Inc., Lincoln, Nebraska) during other periods. This data was used to estimate LAI as a function of canopy height. In

https://doi.org/10.5194/egusphere-2025-3536
Preprint. Discussion started: 4 January 2026

the spring and summer, it was assumed $LAI = 3.25\ H_c$ and in the fall this relationship was assumed to be $LAI = 1.35\ H_c$ due to the drying of the canopy and senescence. Methods for biogeochemical measurements and compensation points for Duke Forest are included in the supplemental material and are described by Walker et al. (2013) for Lillington.

A field-scale box model was developed in the R statistical language that utilizes the same resistance parameterizations and structure as the CMAQ FORTRAN model (see supplemental material). Observed soil and vegetation NH_3 compensation points were set as the median values reported in Walker et al. (2013) and measured at Duke Forest (see supplemental material) and using CMAQ model parameterized values. Latent heat fluxes were estimated by specifying a water vapor stomatal and soil compensation points assuming saturation at the measured leaf and soil temperatures. Fluxes of HNO_3 and SO_2 utilized the same modelling framework with compensation points set to zero for all surface media.

The field-scale model was run for two field campaigns to evaluate its performance in capturing NH_3 and H_2O bidirectional exchange at agricultural and grassland sites and to evaluate its performance in capturing HNO_3 and SO_2 exchange at a grassland site. These simulations utilized the resistance parameterizations indicated here with the exception of the aerodynamic resistance, which was defined as $R_a = Pr_0 \frac{\bar{U}}{u_*^2}$, where Pr_0 is the turbulent Prandtle number (assumed to be 0.95). Note that we are using the measured wind speed and friction velocity and if we were to estimate $\bar{U}$ from u_* the form of R_a presented in Table 1 would be returned. Latent heat fluxes were estimated by assuming that the leaf and soil H_2O compensation points are the saturation vapor pressure at the canopy and soil temperatures, respectively. At Duke Forest, the canopy skin temperature was measured using an infra-red thermometer and at Lillington it was assumed to be the temperature measured by the sonic anemometer mounted closest to canopy level.

2.4 Regional scale application

The model developed by Massad et al. (2010) and Nemitz et al. (2001) with the modifications above is designed to be applied to specific land use types. In the CMAQ v5.3.2 application, this is accomplished by estimating a deposition velocity for each land use type in a grid cell and calculating the grid cell total as an area weighted sum.

$$F_{t,grid} = \sum_{LU=1}^{N_{LU}} f_{LU} F_{t,LU} \tag{19}$$

where, $F_{t,grid}$ is the grid scale flux, LU is the land use index, N_{LU} is the number of land uses in the grid cell, f_{LU} is the ratio of the land use area to total grid area, and $F_{t,LU}$ is the land use specific flux. This scheme makes it necessary to estimate land use specific resistances. This is currently accomplished by applying the land use specific surface roughness length, minimum stomatal resistance, and leaf area index values from the P-X land surface model (Pleim and Xiu, 1995) look up tables in the WRF v4.1.1 model (Skamarock et al., 2019) to recalculate the surface friction velocity and stomatal resistance.

Multiple CMAQ model simulations for the year 2016 were used in this evaluation. Meteorological inputs were from a WRF v4.1.1 simulation using the P-X land surface model, FEST-C model simulations (Ran et al., 2019) were used to provide agricultural data to support the bidirectional exchange model, and emissions were based on the 2016 EMP (Emissions

https://doi.org/10.5194/egusphere-2025-3536
Preprint. Discussion started: 4 January 2026

Modelling Platform: https://www.epa.gov/air-emissions-modeling/2014-2016-version-7-air-emissions-modeling-platforms; Appel et al., 2021) . Additional details regarding the model simulations and CMAQ v5.3.2 model performance with the STAGE deposition option can be found in Appel et al. (2021). In this study, we explore the ammonia bidirectional exchange results and conduct model sensitivities that incorporate observed fertilization rates and observed values for non-agricultural leaf and soil Γ to evaluate the model sensitivity to these factors.

FEST-C model simulations are known to under-estimate annual fertilization rates (Ran et al., 2019). To explore how this model bias impacts CMAQ v5.3.2 ambient NH_3 concentrations and deposition estimates, USDA Economic Research Services (ERS) reported annual fertilizer data was used to post-process FEST-C output for corn, cotton, soybean, and wheat. EPIC fertilizer rates were adjusted by multiplying the grid cell fertilization rate by the ratio of the USDA ERS reported rate over the average FEST-C rate for the state and crop. For states that did not have reported values, the mean ratio of the USDA ERS rate over the mean FEST-C rate for states that had data was used for the adjustment (equation 20). The mean adjustment factor for nitrogen fixing crops, soybeans in this case, and non-nitrogen fixing crops were used to adjust the fertilization rate of these crops respectively.

$$Fert_{adjusted,crop} = max\left(\frac{Fert_{submitted,crop}}{\frac{1}{n_{crop}}\sum Fert_{FEST-C,crop}} Fert_{FEST\quad,crop}, Fert_{max,crop}\right) \quad (20)$$

where $Fert_{adjusted,crop}$ is the FEST-C grid cell adjusted fertilization rate, $Fert_{Submitted,i}$ is the USDA mean annual application data for the specified crop, in kg ha^{-1}, $Fert_{FEST\text{-}C,crop}$ is the initial FEST-C grid cell fertilization rate for the state being considered, n_{crop} is the number of grid cells with fertilization use for the specified crop in the state, and $Fert_{max,crop}$ is the maximum fertilization rate estimated from EPIC for the crop, typically about 300 kg ha^{-1} for a non-nitrogen fixing crop. Nitrification and mineralization rates are captured from FEST-C and evasion rates are estimated using the resistance model above to calculate the nitrogen balance for the modelled soil layers.

2.5 Model Evaluation

At the field scale, hourly modelled fluxes are compared to micrometeorological observations from a fertilized Zea mays field and an unfertilized managed grass field. Mean and median modelled values are evaluated against observations over the complete measurement period for configurations of the box model using parameterizations from the STAGE model in CMAQ v5.3.2 and using field observed values (Table 3).

https://doi.org/10.5194/egusphere-2025-3536
Preprint. Discussion started: 4 January 2026

Table 3. Evaluation of the STAGE model flux estimates compared against Lillington 2007 and Duke Forest 2012 observations. STAGE NH_3 flux estimates are shown with and without a dew water Γ parameterization.

Measurement period	Species	Source of Model Parameters	Mean (Median) Observation	Mean (Median) Model	Normalized Mean (Meidan) Bias	Normalized Mean (Median) Error	Pearson's r (Spearman's ρ)
Lillington 2007	H_2O	CMAQ v5.3.2	69.1 (21.1) W m^{-2}	141.2 (28.7) W m^{-2}	104.4 (53.8) %	106.8 (61.7) %	0.928 (0.933)
Lillington 2007	H_2O	Observed $R_{st,min}$*	-	87.8 (21.7) W m^{-2}	27.0 (24.7)%	36.6 (40.4) %	0.940 (0.936)
Lillington 2007	NH_3	CMAQ v5.3.2	359 (192) ng m^{-2} h^{-1}	503 (390) ng m^{-2} h^{-1}	40.5 (25.1) %	76.4 (80.8) %	0.616 (0.737)
Lillington 2007	NH_3	Observed stomatal and soil Γ, $R_{st,min}$	-	313 (258) ng m^{-2} h^{-1}	-12.6 (9.6) %	61.2 (70.9) %	0.515 (0.651)
Duke Forest 2012	H_2O	CMAQ v5.3.2	29.8 (8.2) W m^{-2}	41.2 (7.1) W m^{-2}	38.6 (12.8) %	96.5 (118.9) %	0.560 (0.720)
Duke Forest 2012	SO_2	CMAQ v5.3.2	-5.8 (-2.7) ng m^{-2} h^{-1}	-5.6 (-1.8) ng m^{-2} h^{-1}	-4.8 (-13.2) %	96.9 (71.0) %	0.411 (0.602)
Duke Forest 2012	HNO_3	CMAQ v5.3.2	-6.2 (-3.1) ng m^{-2} h^{-1}	-7.4 (-3.8) ng m^{-2} h^{-1}	19.3 (12.9) %	61.4 (62.0) %	0.705 (0.792)
Duke Forest 2012	NH_3	CMAQ v5.3.2	8.4 (4.4) ng m^{-2} h^{-1}	-1.5 (-0.9) ng m^{-2} h^{-1}	-117.6 (-143.5) %	118.0 (143.1) %	-0.007 (-0.277)
Duke Forest 2012	NH_3	Observed stomatal and soil Γ	-	8.6 (0.0) ng m^{-2} h^{-1}	2.0 (-55.9) %	125.2 (108.8) %	0.437 (0.451)
Duke Forest 2012 Γ_{ll} (NH_3)	NH_3	Observed stomatal and leaf litter Γ	-	7.7 (-0.2) ng m^{-2} h^{-1}	-8.1 (-67.2) %	127.3 (120.2) %	0.432 (0.313)

* minimum stomatal resistance ($R_{st,min}$)

Evaluation of regional scale results of this model against network observations has been published elsewhere (Appel et al., 2021). Here we focus on the evaluation of the regional scale model estimates against Cross-Track Infrared Sounder (CrIS) satellite observations, Shephard et al. (2020), and estimate the agricultural nitrogen budget and its sensitivity to the parameterization of the NH_3 emission potential.

https://doi.org/10.5194/egusphere-2025-3536
Preprint. Discussion started: 4 January 2026

3 Results and Discussion

3.1 Box Model Evaluation at Field Sites

The STAGE model captured the observed diel variability and magnitude of the HNO_3 and SO_2 fluxes well, Figure 1 and Table 3. The H_2O fluxes at Lillington, NC and Duke Forest, NC were overestimated by the model based on site specific observed values by 27.0% and 38.6%, respectively (Table 3). The error in the Lillington, NC H_2O flux is near the high end of estimated error in eddy covariances fluxes reported by Rannik et al. (2016). The higher error at the Duke Forest site likely represents uncertainty introduced by the lack of LAI and minimum stomatal resistance measurements. The normalized mean bias of the estimated NH_3 flux using mean observed values for the leaf litter and stomatal Γ, -8.1% with a modelled error of 127.3%, was outside the range of reported measurement uncertainty of 31% at the Duke Forest site reported by Rumsey and Walker (2016). The high error was due to outliers skewing the mean. The median modelled fluxes generally underestimated the observed median, Table 3. The diel fluxes indicate that model underestimated nighttime and early morning evasive fluxes and matches midday and afternoon fluxes well, Figure 2b. Sensitivity simulations identified that NH_3 emission potentials for the stomata and ground (represented by leaf litter or soil) can largely explain the biases in the modelled fluxes, Table 3. The median observed leaf litter, Γ_{ll}, soil, Γ_{soil}, and stomatal, $\Gamma_{apoplast}$, NH_3 emission potentials were 144,869, and 2,741 respectively, Table 3. The use of the median measured emission potentials still resulted in absolute biases larger than the observational uncertainty. These measured compensation points are larger than the values parameterized in Massad et al. (2010) used in CMAQ v5.3.2, table 2, and model results using these values at the duke forest site resulted in an averaged -1.3 ng m^{-2} h^{-1} deposition flux while the observed flux was a net emission for the measurement period, Table 3. Model sensitivities at this site show that the modelled fluxes are most sensitive to $\Gamma_{apoplast}$ and our measurements of $\Gamma_{apoplast}$ at this site are similar in magnitude to other studies (e.g. Wang and Schjoerring 2012; Wichink Kruit et al., 2007).

https://doi.org/10.5194/egusphere-2025-3536
Preprint. Discussion started: 4 January 2026

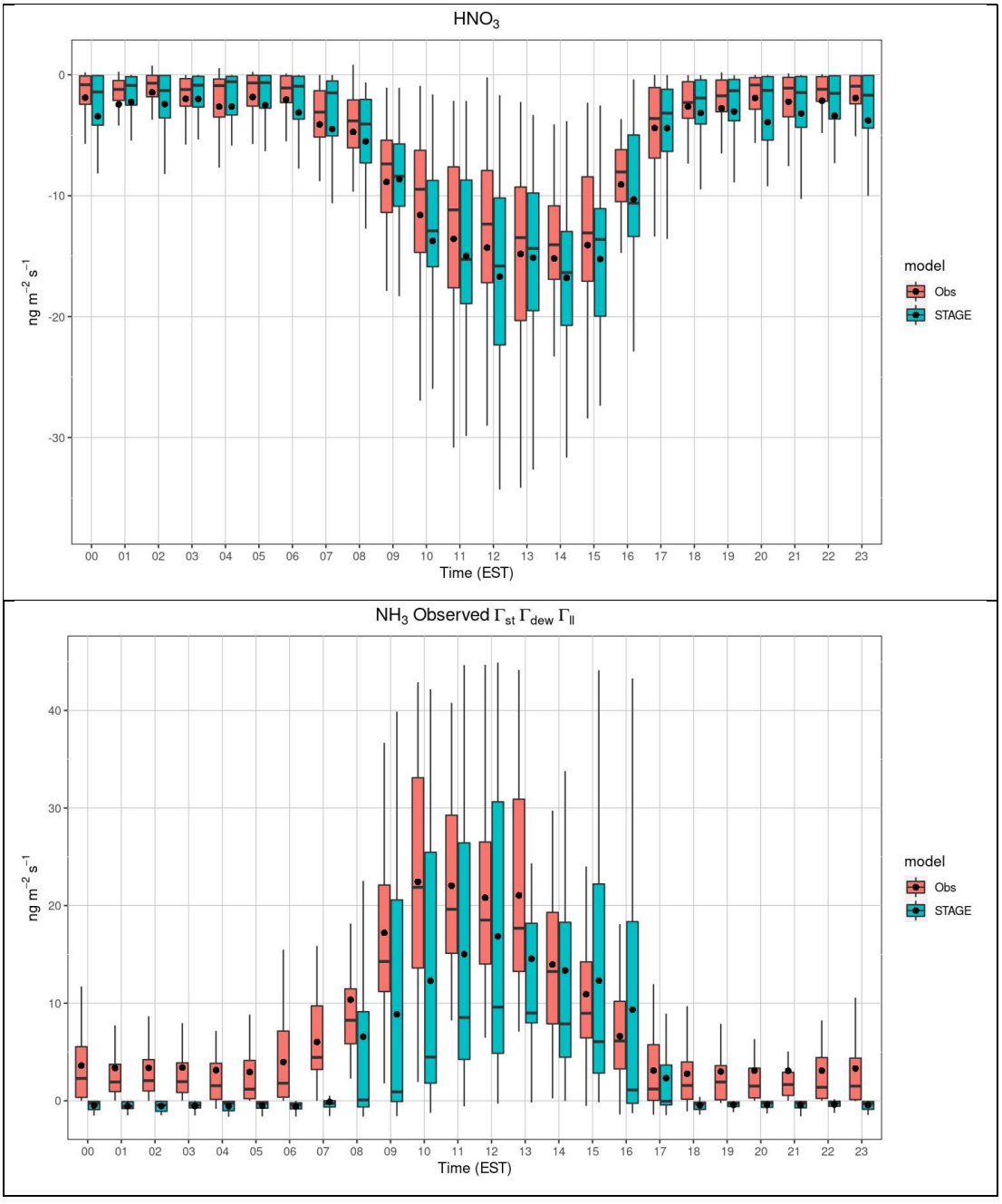

https://doi.org/10.5194/egusphere-2025-3536
Preprint. Discussion started: 4 January 2026

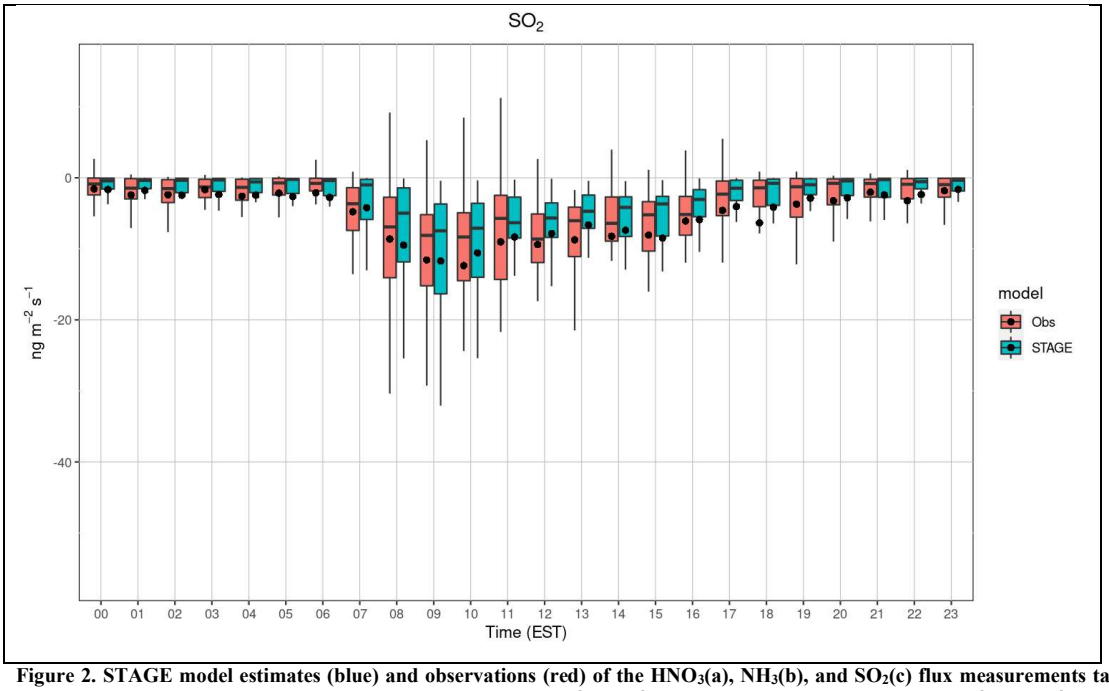

Figure 2. STAGE model estimates (blue) and observations (red) of the HNO_3(a), NH_3(b), and SO_2(c) flux measurements taken at the Duke Forest grasslands flux tower. The box bounds the 25th to 75th percentiles, the lines extend to the 5th and 95th percentile, the black horizontal line is the median and the black point represents the mean of the modelled or observed hourly values. Note that negative values indicate net deposition and positive values indicate net evasion.

The STAGE model captured the magnitude and variability of the observed values at the fertilized corn canopy measured during the Lillington, NC flux campaign with a normalized mean bias of -23.4% when using the median value for the soil NH_4^+ and pH, 31,689.7 µM and 6.43, respectively, and a $\Gamma_{apoplast}$ of 153.5 reported by Walker et al. (2013) and 40.5% when using the CMAQ v5.3.2 parameterizations (Table 3; Figure 3). As noted in Walker et al. (2013), the $\Gamma_{apoplast}$ measurements at this site are much lower than values inferred from micrometeorological measurements, and this may be due to the extraction technique used and/or the growth stage of the crop during which the apoplast chemistry was measured. The modelled NH_3 flux at these sites is most sensitive to the soil and vegetation emission potentials and the model estimates bound both the Lillington and Duke Forest, NC measurements if the median or mean of measured soil emission potentials reported in Walker et al. (2013) and measured at Duke Forest are used.

https://doi.org/10.5194/egusphere-2025-3536
Preprint. Discussion started: 4 January 2026

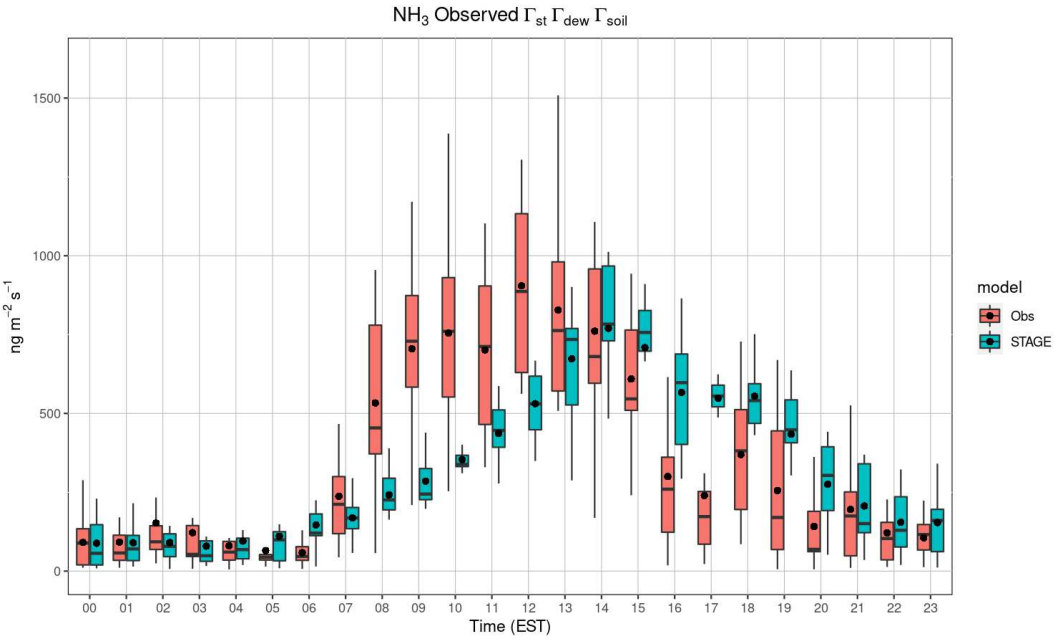

Figure 3, STAGE model estimates (blue) and observations (red) of NH_3 flux measurements taken at the Lillington, NC flux tower over a fertilized corn canopy. The box bounds the 25th to 75th percentiles, the lines extend to the 5th and 95th percentile, the black horizontal line is the median and the black point represents the mean of the modelled or observed hourly values.

These field scale simulations of the Lillington, NC and Duke Forest, NC observations indicate that the STAGE deposition model captures the observed SO_2, HNO_3, and NH_3 fluxes well when measured soil and canopy parameters are used, Table 3. However, when CMAQ v5.3.2 tabular data are used in the simulation the STAGE model fails to capture the magnitude or even the direction of the observed flux. This is the first evaluation of the CMAQ bidirectional NH_3 exchange parameterization against non-agricultural flux observations and indicates that the tabular data in CMAQ v5.3.2 do not reflect the ammonia emission potentials at the Duke Forest, NC field site. The model evaluation at the Lillington, NC agricultural are comparable to previous studies (Pleim et al., 2013). Additional measurements of soil and vegetation, NH_4^+, pH, and NH_3 emission potentials would be beneficial in improving CMAQ model emissions and deposition estimates in non-agricultural regions, approximately 75% of terrestrial surfaces of the 12km conterminous US model domain.

3.2 Regional Scale CMAQ Simulations

Annual ambient NH_3 concentration estimates using the CMAQ modelling system generally capture the magnitude and spatial patterns observed in Cross Infrared Sounder (CrIS) v1.6 (Shephard et al., 2020; Shephard and Cady-Pereira, 2015) satellite observations, Figure 4. Model estimates exceed CrIS observations in the agricultural regions of California, the

https://doi.org/10.5194/egusphere-2025-3536
Preprint. Discussion started: 4 January 2026

Upper Midwest, and Eastern North Carolina and underestimate observations in the Great Plains, the leeward side of the Sierra Nevada's in the Mojave Desert, Eastern Washington, and the agricultural regions of North Central Mexico and coastal ares of Sinaloa Mexico, Figure 4. The mean overestimates in these areas range from 0.5 to 0.9 ppb with maximum overestimates from 7.1 to 9.5 ppb, while mean underestimates at these sites range from -0.6 to -0.62 ppb with maximum underestimates from -2.6 to -3.8 ppb. EPIC fertilization estimates used in CMAQ (Cooter et al., 2012, Bash et al., 2013) only cover the conterminous United States, while values in the Canadian and Mexican portions of the domain use look up tables for agriculture following Zhang et al. (2010) which likely contribute to the observed biases between CMAQ and the CrIS retrievals in Mexico. CMAQ underestimates CrIS NH_3 observations by on the order of 1 ppb over a large swath of non-agricultural land areas, Figure 4. The general CMAQ underestimate of CrIS NH_3 observations in these areas indicates that the CMAQ tabular emission potentials for non-agricultural areas may be generally underestimated as they were for the Duke Forest, NC site. The biases on the leeward side of the Sierra Nevada Mountains where there is little vegetation could be due to the evaporation of NH_4NO_3 aerosols which CMAQ underestimates from the intensive agricultural and urban areas upwind (Kelly et al., 2018) as airmasses undergo adiabatic heating. Currently, we lack ambient NH_3 measurements and measurements of soil and vegetation emission potentials in the Mojave Desert or any other desert regions and can only speculate as to the cause of the model underestimation.

https://doi.org/10.5194/egusphere-2025-3536
Preprint. Discussion started: 4 January 2026

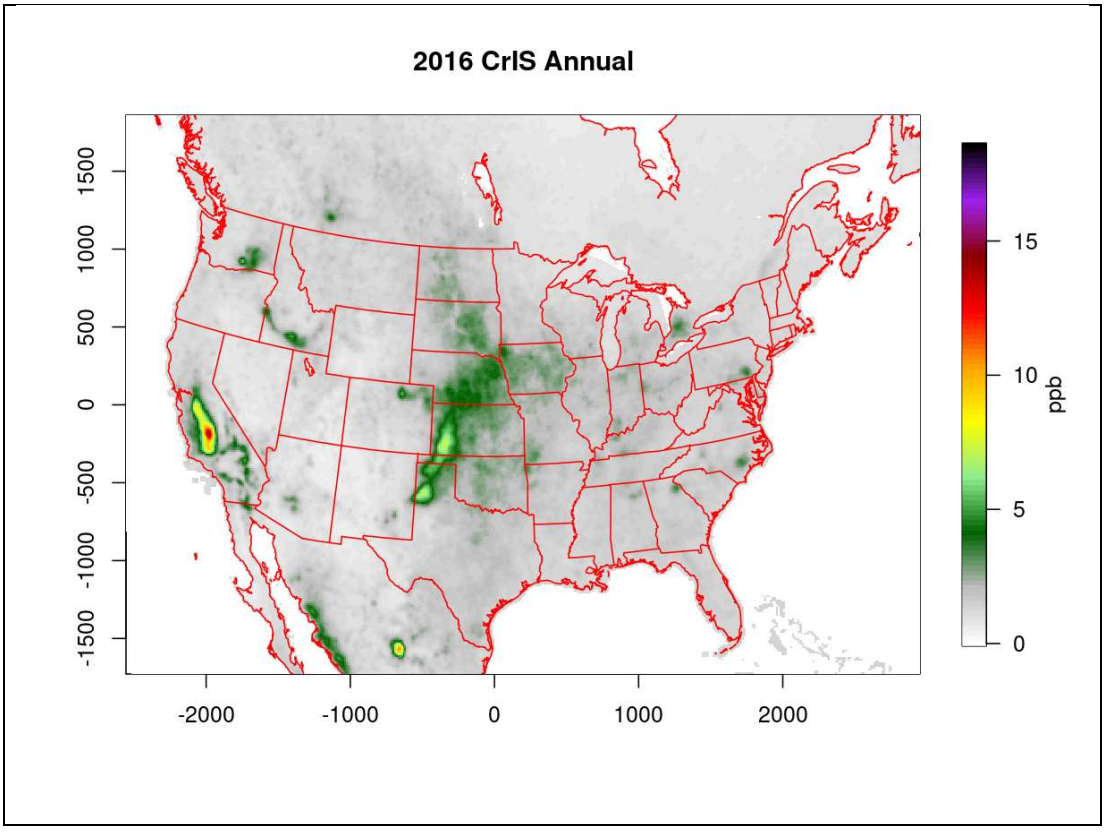

https://doi.org/10.5194/egusphere-2025-3536
Preprint. Discussion started: 4 January 2026

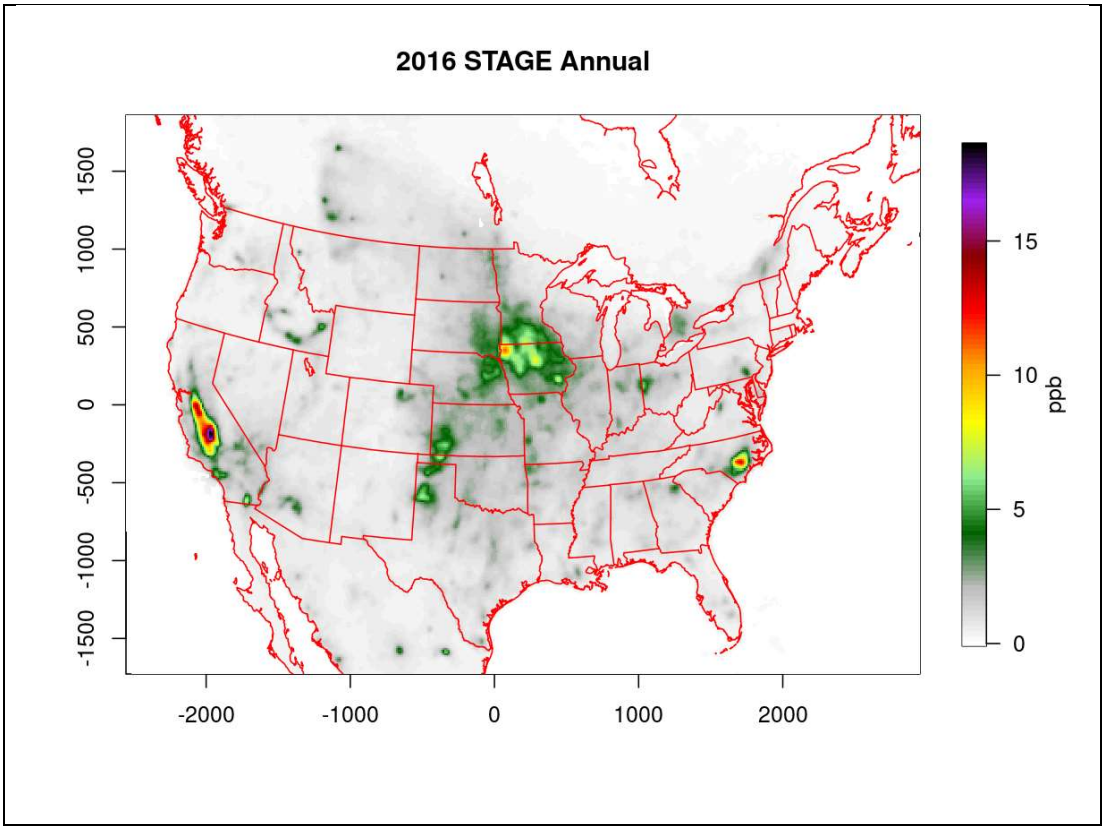

https://doi.org/10.5194/egusphere-2025-3536
Preprint. Discussion started: 4 January 2026

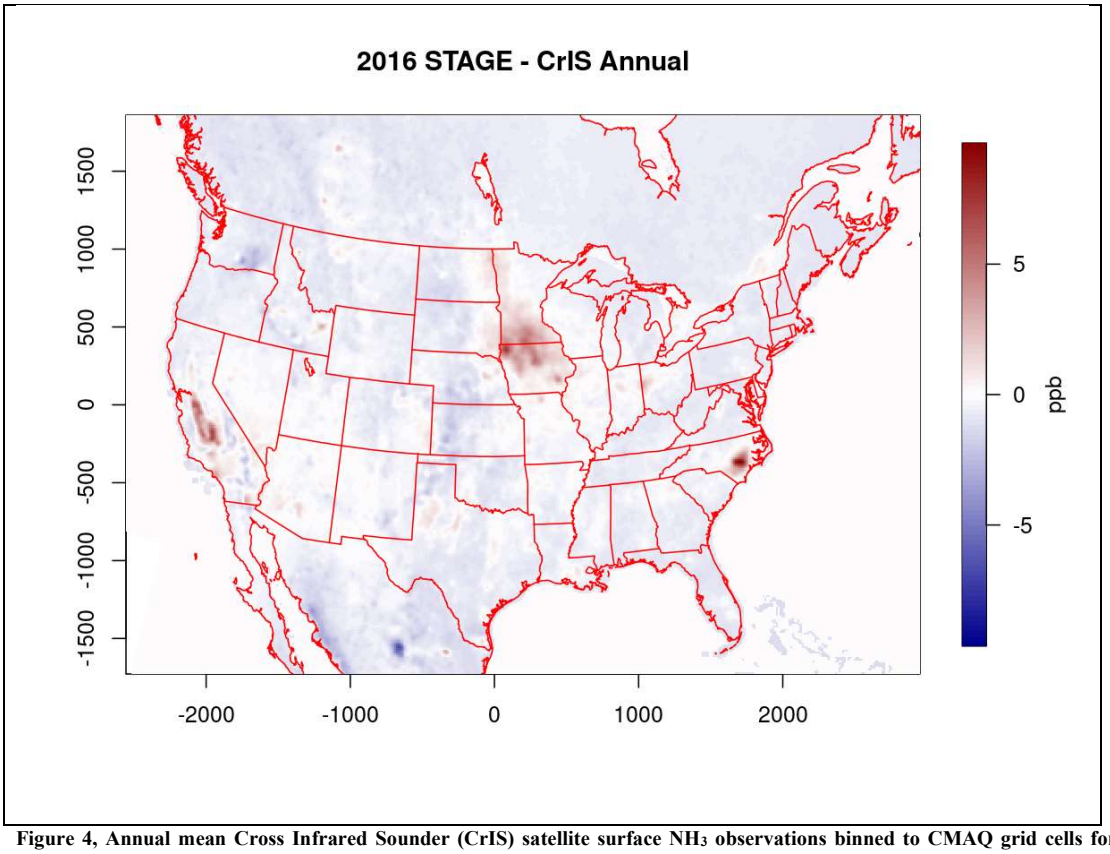

Figure 4, Annual mean Cross Infrared Sounder (CrIS) satellite surface NH_3 observations binned to CMAQ grid cells for 2016 (Top), mean CMAQ surface NH_3 estimates paired in space and time with CrIS observations for 2016 (Middle), the mean difference between CMAQ estimates and CrIS observations of NH_3 paired in space and time for 2016 (Bottom).

The annual regional scale CMAQ model NH_3 biases evaluated against CrIS observations are consistent with the box model simulations, assuming that the results at Lillington, NC and the results from Duke Forest, NC may be generally representative of an agricultural cropping system and grasslands, respectively. Additionally, regional scale model results in the agricultural regions of California and Midwestern U.S. are close to or overestimate the CrIS observations, Figure 3. The magnitude of these regional scale model biases is consistent with the differences between the STAGE box model simulations using CMAQ v5.3.2 tabular data, Table 3. The model biases when compared to CrIS and AMoN sites could largely be eliminated with an increase in the natural NH_3 emission potentials. Approximately a 30% increase in the vegetation emission potential and factor a of 5 increase in the soil surface emission potential would better match the observations at the Duke Forest, NC grasslands sight, Table 2, and likely improve the evaluation against CrIS observations in the Great Plains. While this would represent a relatively large change from the existing values for Γ in CMAQ, this change is also well within the variability of vegetation and soil Γ measurements (Walker et al., 2013; Zhang et al., 2010; Wentworth et al., 2014).

https://doi.org/10.5194/egusphere-2025-3536
Preprint. Discussion started: 4 January 2026

Regional scale evaluations of trace gas deposition rates and processes are currently limited by sparse flux measurement observations. Ambient air-quality monitoring networks and satellite observations can provide an indirect evaluation of dry and wet deposition processes but are often missing key observations need to better constrain model processes, e.g. soil and vegetation NH_3 emission potentials Γ, or particulate matter observations to constrain the impact that aerosol-gas partitioning has on ambient concentrations. Due to the lack of co-located NH_4^+ aerosol observations, our current ability to evaluate NH_3 using satellite and network data are limited to areas where aerosol partitioning processes are likely negligible. Thus, the regional scale CMAQ v5.3.2 evaluation against network (Appel et al., 2021) and CrIS observations best constrain areas that exhibit high NH_3 emissions resulting in high ambient NH_3 concentrations that are less likely to be impacted by modelled errors in NH_4^+. Additionally, the estimated fluxes can be qualitatively evaluated by examining the nitrogen deposition and emission budget against previously published values. Here we tabulate evasion estimates and compare them to fertilizer estimates using the EPIC model (Ran et al., 2019). For the 2016 simulations of Appel et al. (2021), 10.3 MT of N were estimated to be applied as fertilizer to row crops, of that the bidirectional exchange model in CMAQ estimated that 0.5 MT of N, or 4.8% annual emission factor, was estimated to be emitted as NH3 (2017 NEI). An annual NH3 emission factor for mineral fertilizers of 4.8% is within the range of reported values of Klimont and Brink 2004. Deposition values peaked downwind of agricultural sources at approximately 30 kg N ha-1 in Eastern North Carolina, Figure 5, and are well within measured annual deposition values downwind of agricultural sources (Shen et al., 2016) but higher than the net deposition flux of 10 to 16 kg N ha-1 reported by Walker et al. (2014) and Walker et al. (2008) respectively for this region. The CMAQ net NH3 flux is deposition in this area yet CMAQ NH3 concentration estimates are approximately two to three time higher than CrIS observations indicating that NH3 emissions from sources other than bidirectional exchange may be overestimated or CrIS observations are underestimated in Eastern North Carolina.

https://doi.org/10.5194/egusphere-2025-3536
Preprint. Discussion started: 4 January 2026

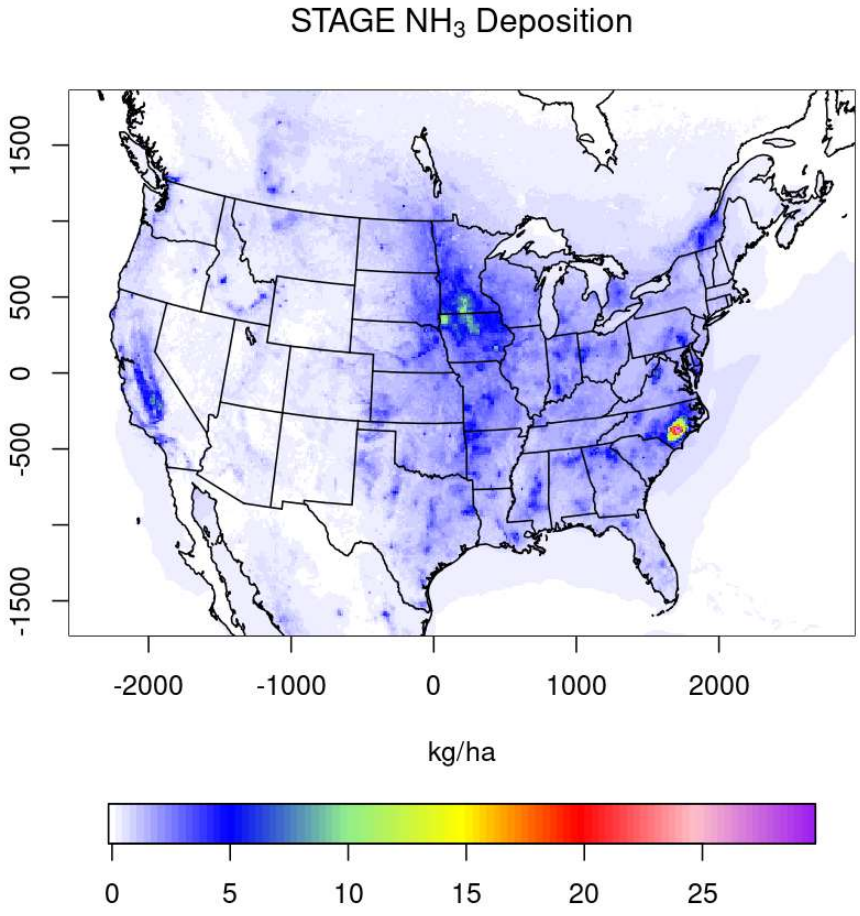

Figure 5, Annual NH_3 dry deposition, in kg N ha^{-1}, for the CMAQ STAGE model simulation evaluated in Appel et al. (2021).

4 Conclusions

A unified dry deposition and bidirectional exchange model was developed for field-scale and CMAQ regional scale models. The STAGE parameterization captured the magnitude and diel variability of observations on the field-scale well when detailed vegetation dynamics and chemistry were available, much like similarly structured field-scale models (Nemitz et al., 2000, Personne et al., 2009, Massad et al., 2010). When implemented in the regional scale CMAQ modelling system, the difference between STAGE and M3Dry (Pleim et al., 2019) deposition models resulted in minor differences in ambient

https://doi.org/10.5194/egusphere-2025-3536
Preprint. Discussion started: 4 January 2026

concentrations of most modelled species with the exception of NH_3 (Appel et al., 2021). This difference is due to the structure of the STAGE model being more similar to that of the non-bidirectional species in the parameterization of Pleim and Ran 2011 than the M3Dry parameterization of NH_3 bidirectional exchange (Pleim *et al.,* 2013).

Parameterization of vegetation and soil ammonium status and its impact on the NH_3 emission potential, Γ, in CMAQ with the STAGE option appears to be the driver of modelled ambient NH_3 biases. On the field-scale, the sensitivity in the modelled NH_3 to soil and vegetation compensation points fall within the variability of the soil and vegetation measurements. On a regional scale, modelled biases are sensitive to the parameterization of soil NH_4 sorption curve and vegetation compensation point. Values of soil and vegetation Γ at the Duke forest site and in recent field-scale measurements (Zhang et al., 2010) indicate that the parameterization used in the STAGE deposition option in CMAQ based on the Massad et al. (2010) annual N deposition fields for non-agricultural land is at the low end of observed vegetation and soil Γ and is likely underestimating the variability and magnitude of soil and vegetation compensation points, particularly for grasslands (Mattsson et al., 2009; Zhang et al., 2010; Wentworth et al., 2014). The evaluation against CrIS NH_3 observations shows that the magnitude and spatial patterns in the concentration fields are captured well in CMAQ simulations but ambient concentrations are overestimated in some predominantly agricultural areas. The regional scale model underestimates ambient NH_3 in non-agricultural largely vegetated areas when compared to CrIS observations, Figure 3. This is in general agreement with the differences in the soil sorption parameters in the Venterea et al. (2015) model and leaf and vegetation NH_3 emissions potential parameters measured at Lillington and Duke Forest, NC and the tabular values for soil and vegetation emission potentials in CMAQ, Tables 2 and 3. The magnitude of the CMAQ modelled NH_3 bias against CrIS observations using the STAGE surface exchange option, typically less than 1 μg m^{-3}, can largely be explained by the differences in the tabular values used in CMAQ and the observed values reported here and in other studies (e.g. Zhang et al., 2010) and indicates that nitrogen cycling in the natural environment implicated in the Duke Forest flux measurements (Rumsey et al., 2016) is greater than in the current CMAQ v5.3.2 parameterization. The general sensitivity of the STAGE model to the soil and vegetation emission potentials indicates that regional scale model results for NH_3 can be further improved with additional micrometeorological flux measurements and additional measurements of the vegetation and soil chemistry over different land use types, soil types, and vegetation phenological stages.

Author Contributions

JOB developed the model air-surface exchange code and performed model sensitivity simulations. Base model simulations were conducted and shared by KWA. Flux and environmental media measurements were conducted by JWT, ZW, ICR, MRJ, and NIA. The initial draft was written by JOB with substantial contributions documenting the observations from JWT, ICR, and MRJ. ZW, BM, CH, KMF, and HOTP provided guidance in the development of the model code and analysis. MS and KEC-P provided CrIS observations. All co-authors contributed to the editing and revisions of this manuscript.

https://doi.org/10.5194/egusphere-2025-3536
Preprint. Discussion started: 4 January 2026

Code Availability

The STAGE deposition option is within CMAQv5.3.2, which is available at https://doi.org/10.5281/zenodo.4081737 (U.S. EPA, 2020b).

Data Availability

Hourly observed meteorological data, observed flux data and CMAQ modelled flux data at Duke Forest, NC and Lillington NC are available in the supplementary material. Regional scale CMAQ model results are available upon request from KWA. CrIS observations are available upon request from MS.

Competing Interests

The authors have no other competing interests to declare.

Disclaimer

The views expressed in this document are solely those of the authors and do not necessarily reflect those of the U.S. EPA.

References

Alnsour, Najwa, 2020. Bi-directional exchange of ammonia from soils in row crop agro-ecosystems. Dissertation. North Carolina State University. http://www.lib.ncsu.edu/resolver/1840.20/37245

Appel, K. W., Bash, J. O., Fahey, K. M., Foley, K. M., Gilliam, R. C., Hogrefe, C., Hutzell, W. T., Kang, D., Mathur, R., Murphy, B. N., Napelenok, S. L., Nolte, C. G., Pleim, J. E., Pouliot, G. A., Pye, H. O. T., Ran, L., Roselle, S. J., Sarwar, G., Schwede, D. B., Sidi, F. I., Spero, T. L., and Wong, D. C., The Community Multiscale Air Quality (CMAQ) model versions 5.3 and 5.3.1: system updates and evaluation, Geosci. Model Dev., 14, 2867–2897, https://doi.org/10.5194/gmd-14-2867-2021, 2021

Barthlott, W., Mail, M., Neinhuis C., Superhydrophobic hierarchically structured surfaces in biology: evolution, structural principles and biomimetic applications. Phil. Trans. R. Soc. A. 374:20160191, https://doi.org/10.1098/rsta.2016.0191, 2016

Bash, J.O., Cooter, E.J., Dennis. R.W., Walker, J.T., Pleim. J.E., Evaluation of a regional air-quality model with bi-directional NH3 exchange coupled to an agro-ecosystem model, Biogeosciences, 10, 1635-1645, 2013

Bash, J.O., Walker, J.T., Katul, G.G., Jones, M.R., Nemitz, E., Robarge, W.P., Estimation of in-canopy ammonia sources and sinks in a fertilized Zea mays field, Environ. Sci. Technol., 44, 1683-1689, 2010

Brunauer, S., Emmett, P.H., Teller, E., Absorption of gases in multimolecular layers, J. Am. Chem. Soc., 60(2), 309-319, doi:10.1021/ja01269a023, 1938

Burkhardt, J., Flechard, C.R., Gresens, F., Mattsson, M., Jongejan, P.A.C., Erisman, J.W., Weidinger, T., Meszaros, R., Nemitz, E., Sutton, M.A.: Modeling the dynamic chemical interactions of atmospheric ammonia with leaf surface wetness in a managed grassland canopy, Biogeosci. 6, 67-84, https://doi.org/10.5194/bg-6-67-2009, 2009

Burnett, R., Chen, H., Szyszkowicz, M., Fann, N. Hubbell, B., Pope, C.A., Apte, J.S., Brauer, M., Cohen, A., Weichenthal, S., Coggins, J., Di, Q., Brunekreef, B., Frostad, J., Lim, S.S., Kan, H., Walker, K.D., Thurston, G.D., Hayes, R.B., Lim., C.C., Turner, M.C., Jerrett, M.,

https://doi.org/10.5194/egusphere-2025-3536
Preprint. Discussion started: 4 January 2026

Krewski, D., Gapstur, S.M., Diver, W.R., Ostro, B., Goldberg, D., Crouse, D.L., Martin, R.V., Peters, P., Pinault, L., Tjepkema, M., van Donkelaar, A., Villeneuve, P.J., Miller, A.B., Yin, P., Zhou, M., Wang, L., Janssen, N.A.H., Marra, M., Atkinson, R.W., Tsang, H., Thack, T.Q., Cannon, J.B., Allen R.T., Hart, J.E., Laden, F., Cesarone, G., Forastiere, F., Weinmayr, G., Jaensch, A., Nagel, G., Concin, H., Spadaro, J.V.: Global estimates of mortality associated with long term exposure to outdoor fine particulate matter, Proc. Nat. Academy Sci. 115(38), 9592-9597, http://dx.doi.org/10.1073/pnas.1803222115, 2018

Byrne, A.; The 1979 convention on long-range transboundary air pollution: assessing its effectiveness as a multilateral environmental regime after 35 years. Transnational Environ. Law 4 (01), 37–67. http://dx.doi.org/10.1017/s2047102514000296, 2015

Clifton, O.E., Paulot, F., Fiore, A.M., Horowitz, L.W., Correa, G., Baublitz, C.B., Fares, S., Goded, I., Goldstein, A.H., Gruening, C., Hogg, A.J., Loubet, B., Mammarella, I., Munger, J.W., Neil, L., Stella, P., Uddling, J., Vesla, T., Weng, E.: Influence of dynamic ozone dry deposition on ozone pollution, J. Geophys. Res. Atmos. 125, e2020JD032398, doi:10.1029/2020JD032398, 2020

D'Ambro, E.L., Pye, H.O.T., Bash, J.O., Bowyer, J., Allen, C., Efstathiou, C., Gilliam, R.C., Reynolds, L., Talgo, K., Murphy, B.N.; Characterizing the Air Emissions, Transport, and Deposition of Per- and Polyfluoroalkyl Substances from a Fluoropolymer Manufacturing Facility, Environmental Science & Technology 55 (2), 862-870, DOI: 10.1021/acs.est.0c06580, 2021

Eschleman, K.N., Sabo, R.D., Declining nitrate-N yields in the Upper Potomac River Basin, What is realy driving progress under the Chesapeake Bay restoration? Atmos. Environ. 146, 280-289, doi:10.1016/j.atmosenv.2016.07.004, 2016

Fahey, K. M., Carlton, A. G., Pye, H. O. T., Baek, J., Hutzell, W. T., Stanier, C. O., Baker, K. R., Appel, K. W., Jaoui, M., and Offenberg, J. H.: A framework for expanding aqueous chemistry in the Community Multiscale Air Quality (CMAQ) model version 5.1, Geosci. Model Dev., 10, 1587-1605, 2017.

Galloway, J. E.; Moreno, A. V. P.; Lindstrom, A. B.; Strynar, M. J.; Newton, S.; May, A. A.; Weavers, L. K. Evidence of Air Dispersion: HFPO−DA and PFOA in Ohio and West Virginia Surface Water and Soil near a Fluoropolymer Production Facility. Environ. Sci. Technol., 54, 7175−7184, 2020

Galmarini, S., Makar, P., Clifton, O.E., Hogrefe, C., Bash, J.O., Bellasio, R., Bionconi, R., Bieser, J., Butler, T., Ducker, J., Flemming, J., Hodzic, A., Holmes, C.D., Kioutsioukis, I., Kranenburg, R., Lupascu, A., Perez-Camanyo, J.L., Pleim, J., Ryu, Y.-H., San Jose, R., Schwede, D., Silva, S., Wolke, R., Technical note: AQMEII4 Activity 1: evaluation of wet and dry deposition schemes as an integral part of regional-scale air quality models., Atmos. Chem. Phys., 21, 15663-15697, doi:10.5194/acp-21-15663-2021, 2021

Greaver, T.L., Sullivan, T.J., Herrick, J.D., Barber, M.C., Baron, J.J., Cosby, B.J., Deerhake, M.E., Dennis, R.L., Dubois, J.-J.,B., Goodale, C.L., Herlihy, A.T., Lawrence, G.B., Lio, L., Lynch, J.A., Novak, K.J.; Ecological effects of nitrogen and sulfur air pollution in the US: what do we know?, Front. Ecol. Environ., 10(7), 365-372, doi:10.1890/110049, 2012

Hansen, K., Personne, E., Skjøth, Loubet, B., Ibron, A., Jensen, R., Sørensen, L.L., Investigating sources of measured forest-atmosphere ammonia fluxes using two layer bi-directional modelling, Ag. Forest Meteor. 237-238, 80-94, http://dx.doi.org/10.1016/j.agrformet.2017.02.008, 2017

Van Hove, L.W.A., Adema, E.H.: The effective thickness of water films on leaves, Atmos. Environ., 30, 2933-2936, https://doi.org/10.1016/1352-2310(96)00012-X, 1996

Hummelshøj, P., Jensen, N.O.: Derivation of canopy resistance for water vapour fluxes over a spruce forest, using a new technique for the viscous sublayer resistance, Ag. Forest Meteor. 73, 339-352, https://doi.org/10.1016/0168-1923(94)05083-I, 1995

Jetter, R., Riederer, M., Localization of the transpiration barrier in the epi- and intracuticular waxes of eight plant species: water transport resistances are associated with fatty acyl rather than alicyclic components, Plant Physiology, 170, 921-934, https://doi.org/10.1104/pp.15.01699, 2016

Jetter, R., Riederer, M.: Epicuticular crystals of nonacosan-10-ol: In-vitro reconstitution and factors influencing cystal habits, Planta, 195, 257-270, 1994

Kelly, J.T., Parworth, C.L., Zhang, Q., Miller, D.J., Sun, K., Zondlo, M.A., Baker, K.R., Wisthaler, A., Nowak, J.B., Pusede, S.E., Cohen, R.C., Weinheimer, A.J., Beyersdorf, A.J., Tonnesen, G.S., Bash, J.O., Valen, L.C., Crawford, J.H., Fried, A., Walega, J.G., Modeling NH4NO3 over the San Joaquin Valley durning the 2012 DISCOVER-AQ campaign, J. Geophys. Res. Atmos., 123, 4727-4745, https://doi.org/10.1029/2018JD028290, 2018

Klimont, Z., Brink, C. Modeling of Emissions of Air Pollutants and Greenhouse Gases from Agricultural Sources in Europe. IIASA Interim Report. IIASA, Laxenburg, Austria: IR-04-048, 2004

Liss, P.S., Slater, P.G.: Fluxes of gases across the air-sea interface, Nature, 247, 181-184, https://doi.org/10.1038/247181a0, 1974

https://doi.org/10.5194/egusphere-2025-3536
Preprint. Discussion started: 4 January 2026

Massad, R-S., Nemitz, E., Sutton, M.A., Review and parameterization of bi-directional ammonia exchange between vegetation and the atmosphere, Atmos. Chem. Phys., 10, 10359-10386, 2010

Mattsson, M., Herrmann, B., David, M., Loubet, B., Riedo, M., Theobald, M. R., Sutton, M. A., Bruhn, D., Neftel, A., and Schjoerring, J. K.: Temporal variability in bioassays of the stomatal ammonia compensation point in relation to plant and soil nitrogen parameters in intensively managed grassland, Biogeosciences, 6, 171–179, https://doi.org/10.5194/bg-6-171-2009, 2009.

Meyers, T. P., Hall, M. E., Lindberg, S. E., and Kim, K.: Use of the modified Bowen-ratio technique to measure fluxes of trace gases, Atmos. Environ., 30, 3321 – 3329, 1996.

Millet, D.B., Alwe, H.D., Chen, X., Deventer, M.J., Griffis, T.J., Holzinger, R.,Bertman, S.B., Rickly, P.S., Stevens, P.S., Léonardis, T., Locoge, N., Dusanter, S., Tyndall, G.S., Alvarez, S.L., Erickson, M.H., Flynn, J.H., Bidirecitional ecosystem-atmosphere fluxes of volatile organic compounds across the mass spectrum. How many matter? Envrion. Sci. Tech. 2018, 2 (8), 764-777, https://doi.org/10.1021/acsearthspacechem.8b00061, 2018.

Nemitz, E., Milford, C., and Sutton, M. A.: A two-layer canopy compensation point model for describing bi-directional biosphere-atmosphere exchange of ammonia, Q. J. Roy. Meteor. Soc., 127, 815–833, 2001.

Olaguer, E.P. Atmospheric Impacts of the Oil and Gas Industry; Elsevier: New York, NY, USA, 2017; ISBN 978-0-12-801883-5

Personne, E., Loubet, B., Herrmann, B., Mattson, M., Schjoerring, J.K., Nemitz, E., Sutton, M.A., Cellier, P., SURFATM-NH3: a model combining the surface energy balance and bi-directional exchanges of ammonia applied to a field-scale, Biogeosci. 6, 1371-1388, doi:10.5194/bg-6-1371-2009, 2009

Pleim, J.E., Xiu, A., Development and testing of a surface flux and planetary boundary layer model for applications in mesoscale models, J. Appl. Meteor. 34(1), 16-32, https://doi.org/10.1175/1520-0450-34.1.16, 1995

Pleim, J.E., Ran, L.-R., Surface flux modeling for air quality applications, Atmosphere, 2, 271-302, https://doi.org/10.3390/atmos2030271, 2011

Pleim, J. E., Bash, J. O., Walker, J. T., Cooter, E. J.: Development and testing of an ammonia bi-directional flux model for air-quality models, J. Geophys. Res. Atmos., 118, https://doi.org/10.1002/jgrd.50262, 2013.

Pleim, J. E., Ran, L., Appel, W., Shephard, M. W., and Cady-Pereira, K.: New bidirectional ammonia flux model in an air quality model coupled with an agricultural model. J. Adv. Model Earth Syst., 11 (9), 2934-2957, https://doi.org/10.1029/2019MS001728, 2019.

Ran, L., Yuan, Y., Cooter, E., Benson, V., Yang, D., Pleim, J., Wang, R. and Williams, J.: An integrated agriculture, atmosphere, and hydrology modeling system for ecosystem assessments. Journal of Advances in Modeling Earth Systems, 11 (12), 4645-4668, https://doi.org/10.1029/2019MS001708, 2019.

Rannik, Ü., Peltola, O., Mammarella, I., Random uncertainties of flux measurements by the eddy covariance technique, Atmos. Meas. Tech., 9, 5163-5181, doi:10.5194/amt-9-5163-2016, 2016

Raupach, M.R., Applying Lagrangian fluid mechanics to infer scalar source distributions from concentration profiles in plant canopies, Agric. For. Meteorol., 47, 85-108, 1989

Rumsey, I.C., Walker, J.T.: Application of an online ion-chromatography-based instrument for gradient flux measurements of speciated nitrogen and sulfur, Atmos. Meas. Tech. 9, 2581-2592, doi:10.5194/amt-9-2581-2016, 2016

Rumsey, I., Cowen, K., Walker, J.T., Kelley, T.J., Hanft, E.A., Mishoe, K., Rogers, C., Proost, R., Beachley, G.M., Lear, G., Frelink, T., Otjes, R.P. An assessment of the performance of the Monitor for AeRosols and GAses in ambient air (MARGA): a semi-continuous method for soluble compounds. Atmos. Chem. Phys., 14 (11), 5639–5658, DOI 10.5194/acp-14-5639-2014, 2014.

Schrader, F., Brümmer, C.: Land use specific ammonia deposition velocities: a review of recent studies (2004-2013), Water Air Soil Pollut. 225(10), 2114, https://dx.doi.org/10.1007%2Fs11270-014-2114-7, 2014

Schreiber, L., and Schoenherr, J.: Water and solute permeabilities of plant cuticles: measurements and data analysis, Springer, 299 pp, 2009.

Shephard, M. W. and Cady-Pereira, K. E.: Cross-track Infrared Sounder (CrIS) satellite observations of tropospheric ammonia, Atmos. Meas. Tech., 8, 1323–1336, https://doi.org/10.5194/amt-8-1323-2015, 2015.

Shephard, M. W., Dammers, E., Cady-Pereira, K. E., Kharol, S. K., Thompson, J., Gainariu-Matz, Y., Zhang, J., McLinden, C. A., Kovachik, A., Moran, M., Bittman, S., Sioris, C. E., Griffin, D., Alvarado, M. J., Lonsdale, C., Savic-Jovcic, V., and Zheng, Q.: Ammonia

https://doi.org/10.5194/egusphere-2025-3536
Preprint. Discussion started: 4 January 2026

measurements from space with the Cross-track Infrared Sounder: characteristics and applications, Atmos. Chem. Phys., 20, 2277–2302, https://doi.org/10.5194/acp-20-2277-2020, 2020

Seinfeld, J.H., and Pandis, S.N.: Atmospheric chemistry and physics: from air pollution to climate change, John Wiley & Sons Inc. New York, 1998

Skamarock, W.C., Klemp, J.B., Dudhia, J., Gill, D.O., Liu, X., Berner, J., Wang, W., Powers, J.G., Duda, M.G., Barker, D.M., Huang, X.-Y., A Description of the advanced research WRF version 4., NCAR Tech. Note NCAR/TN-556+STR, 145 pp. doi:10.5065/1dfh-6p97, 2019

Skiba, U., Sheppard, L., Pitcairn, C.E.R., Leith, I., Crossley, A., van Dijk, S., Kennedy, V.H., Fowler D.: Soil nitrous oxide and nitric oxide emissions as indicators of elevated atmospheric N deposition rates in seminatural ecosystems, Environmental Pollution, 102(1), 457-461, https://doi.org/10.1016/S0269-7491(98)80069-9, 1999

Shuttleworth, W.J., Wallace, J.S., Evaporation from sparse crops – an energy combination theory, Q. J. Roy. Meteor. Soc, 111, 839-855, 1985

Stella, P., Personnne, E., Loubet, B., Lamaud, E., Ceschia, E., Béziat, P., Bonnefond, J.M., Irvine, M., Keravec, P., Mascher, N., Cellier, P., Predicting and portioning ozone fluxes to maize crops from sowing to harvest: the Surfatm-O3 model, Biogeosci. 8, 2869-2886, doi:10.5194/bg-8-2869-2011, 2011

Swenson, S.C., Lawrence, D.M., Assessing a dry surface layer-based soil resistance parameterization for the Community Land Model using GRACE and FLUXNET-MTE data, J. Geophys. Res. Atmos. 199(17), https://doi.org/10.1002/2014JD022314, 2014Thomas, R.M., Trebs, I., Otjes, R., Jongejan, P.A.C., ten Brink, H., Phillips, G., Kortner, M., Meixner, F.X., Nemitz, E. An automated analyzer to measure surface-atmosphere exchange fluxes of water soluble inorganic aerosol compounds and reactive trace gases. Environ. Sci. Technol., 43 (5), 1412-1418, DOI 10.1021/es8019403, 2009.

U.S. Congress. United States Congress. Clean Water Act Amendments of 1972. P.L. 92-500. U.S. Government Printing Office, Washington, DC., 1972

U.S. Congress. United States Congress. Clean Air Act Amendments of 1990. P.L. 101-549. U.S. Government Printing Office, Washington, DC., 1990

U.S. EPA, 2020a. Integrated Science Assessment (ISA) for Oxides of Nitrogen, Oides of Sulfur and Particulate Matter Ecological Criteria (Final Report), U.S. Environmental Protection Agency, Washington, D.C., EPA/60/R-20/278, 2020

U.S. EPA, 2020b. Community Multiscale Air Quality (CMAQ) model v5.3.2. https://doi.org/10.5281/zenodo.4081737 (accessed July 16, 2025).

Venterea, R.T., Clough, T.J., Coulter, J.A., Breuillin-Sessoms, F., Wang, P., Sadowsky, M.J., Ammonium sorption and ammonia inhabitation of nitrate-oxidizing bacteria explain contrasting soil N2O production, Sci. Rep., 5, 12513 doi:10.1038/srep12153, 2015

Walker, J.T., Jones, M.R., Bash, J.O., Myles, L., Meyers, T., Schwede, D., Herrick, J., Nemitz, E., Robarge, W,. Processes of ammonia air-surface exchange in a fertilized Zea mays canopy. Biogeosciences, 10, 981-998., 2013

Walker, J.T., Austin, R., Robarge, W.P. 2014. Modeling of ammonia deposition to a Pocosin landscape downwind of a large poultry facility. Agriculture, Ecosystem, and Environment, 185, 161-175.

Walker, J.T., Spence, P., Kimbrough, S., Robarge, W. 2008. Inferential model estimates of ammonia dry deposition in the vicinity of a swine production facility. Atmospheric Environment, 42, 3407-3418Wang, X., Lin, C.-J., and Feng, X.: Sensitivity analysis of an updated bidirectional air–surface exchange model for elemental mercury vapor, Atmos. Chem. Phys., 14, 6273–6287, https://doi.org/10.5194/acp-14-6273-2014, 2014

Wentworth, G. R., Murphy, J. G., Gregoire, P. K., Cheyne, C. A. L., Tevlin, A. G., and Hems, R.: Soil–atmosphere exchange of ammonia in a non-fertilized grassland: measured emission potentials and inferred fluxes, Biogeosciences, 11, 5675–5686, https://doi.org/10.5194/bg-11-5675-2014, 2014.

Wichink Kruit, R. J., van Pul, W. A. J., Otjes, R. P., Hofschreuder, P., Jacobs, A. F. G., and Holtslag, A. A. M.: Ammonia fluxes and derived canopy compensation points over non-fertilised agricultural grassland in The Netherlands using the new gradient ammonia – high accuracy – monitor (GRAHAM), Atmos. Environ., 41, 1275–1287, 2007.

Wichink Kruit, R. J., Schaap, M., Souter, F.J., van Zanten, M.C., van Pul, W.A.J.: Modeling the distribution of ammonia across Europe including bi-directional surface-atmosphere exchange, Biogeosci., 9, 5261-5277, doi:10.5194/bg-9-5261-2012, 2012

https://doi.org/10.5194/egusphere-2025-3536
Preprint. Discussion started: 4 January 2026

Wolfe, G. M. and Thornton, J. A.: The Chemistry of Atmosphere-Forest Exchange (CAFE) Model – Part 1: Model description and characterization, Atmos. Chem. Phys., 11, 77–101, https://doi.org/10.5194/acp-11-77-2011, 2011

Wu, D., Horn, M.A., Behrendt, T. et al. Soil HONO emissions at high moisture content are driven by microbial nitrate reduction to nitrite: tackling the HONO puzzle. ISME J 13, 1688–1699. https://doi.org/10.1038/s41396-019-0379-y, 2019

Yi, C.: Momentum transfer within canopies, J. Appl. Meteorol. Climatol., 47, 262-275, 2008.

Zhang, L., Wright, L. P., and Asman, W. A. H.: Bi-directional air surface exchange of atmospheric ammonia: a review of measurements and a development of a big-leaf model for applications in regional-scale air-quality models, J. Geophys. Res., 115, D20310, doi:10.1029/2009JD013589, 2010